EXCHANGE CURRENTS IN RADIATIVE HYPERON DECAYS AND HYPERON CHARGE RADII

GEORG WAGNER

Institut für Theoretische Physik, Universität Tübingen, Auf der Morgenstelle 14, 72076 Tübingen, Germany

Radiative decays of decuplet hyperons and octet hyperon charge radii are evaluated in a chiral constituent quark model emphasizing the role of exchange currents. Exchange currents largely cancel for the M1 decay amplitudes, while they dominate the E2 amplitude. Due to the pseudoscalar meson cloud the charge radii of Σ^- and Ξ^- are almost as large as the proton radius, in agreement with recent experimental results from SELEX. Strangeness suppression is weakened by exchange currents for several observables.

1 Introduction

In this contribution we summarize our analysis of exchange current effects in the radiative hyperon decays[1] and in octet hyperon charge radii[2]. With the advent of new facilities, detailed measurements of the radiative decays of some Σ^* and Ξ^* hyperons[3] are under way. Charge radii of some hyperons are now under experimental investigation[4], too. Many model calculations of hyperon decays (see Ref. list in[1]) and electromagnetic radii (see Ref. list in[2]) are available for comparison.

The reasons for increased interest in these observables are twofold. The $E2/M1$ ratios in the radiative hyperon decays contain information on deformations, if not of the valence quarks, then of the non-valence-quark distributions in the baryons. Second, the observables are sensitive to $\mathrm{SU}_F(3)$ flavor symmetry breaking and strangeness suppression. Therefore, comparison of model predictions with experiment may pin down the relevant non-valence degrees of freedom in the effective quark-quark interaction.

2 Exchange currents in the chiral constituent quark model

Constituent quarks emerge as the effective quasi-particle degrees of freedom in low-energy QCD due to the spontaneously broken chiral symmetry. In our non-relativistic realisation of the chiral quark model a two-body confinement potential is used. The pseudoscalar (PS) meson octet, that constitute the Goldstone bosons of the symmetry breaking, provide the intermediate range interactions between quarks. At short range, residual one-gluon exchange is included. For the baryon wave functions we use spherical $(0s)^3$ oscillator states

and $SU_{SF}(6)$ spin-flavor states. A detailed discussion of the Hamiltonian, parameters, wave functions, hyperon masses and magnetic moments can be found in Ref.[5].

Guided by the continuity equation, the electromagnetic currents to be considered for the above described Hamiltonian are constructed[5,6] by a non-relativistic reduction of the relevant Feynman diagrams shown in Figure 1.

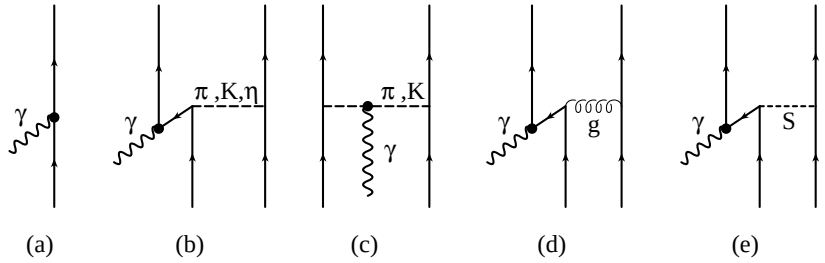

Figure 1. Electromagnetic one- and two-body currents as required by the continuity equation. (a) Impulse approximation, (b) PS-meson pair current (π, K, η), (c) PS-meson in-flight current (π, K), (d) gluon-pair current, and (e) scalar exchange current (i.e. confinement).

3 Radiative hyperon decays

Table 1 collects our results on the radiative decays of decuplet hyperons[1]. Individual exchange current contributions to the $M1$ transition moments can be as large as 60% of the impulse approximation. However overall, like for the octet baryon magnetic moments[5], exchange currents provide less than 10% corrections to the impulse approximation results. Strangeness suppression in impulse approximation, i.e. in the valence quark picture, is considerable due to $m_u/m_s \simeq 0.6$ (first column in Table 1). Strangeness suppression is for all six strange decays reduced when exchange currents are included. The transition magnetic moments for the negatively charged hyperons deviate considerably from the $SU_F(3)$ flavor-symmetric value 0.

The transition quadrupole moments Q shown in Table 1 receive large contributions from the PS-meson and gluon-pair diagrams, Figs. 1(b) and 1(d). The $E2$ moments would be zero in impulse approximation for spherical valence quark configurations. The dynamical origin for the allowed exchange current contributions is a double spin-flip transition[6] of the two quarks involved. The gluon contributes strongly to most transition quadrupole moments, on the average $\sim 2/3$ of the total $E2$ moment. The experimental results may give important hints on the relevance of effective gluon degrees of freedom in hadron properties.

The decay width $\Gamma \propto |A_{3/2}|^2 + |A_{1/2}|^2$ is related to the helicity amplitudes $A_{3/2}$ and $A_{1/2}$, which can be expressed as linear combinations of the $M1$ and $E2$ transition formfactors[6]. The $E2/M1$ ratio of the transition amplitudes is commonly defined as $E2/M1 = \frac{\omega M_N}{6} Q/\mu$ with the resonance frequency ω. Due to cancellations of exchange current contributions to the $M1$ transition amplitude and the relative smallness of the $E2$ amplitude, the decay widths Γ are dominated by the $M1$ impulse approximation. Only restricted informations on non-valence quark effects should be expected from the experiments here, similar to the situation for octet magnetic moments.

All model calculations yield large (the largest) $E2/M1$ ratios for negatively charged states. The $E2/M1$ ratio for the decays of negatively charged hyperons are particularly model dependent[1] due to the smallness of both the $E2$ and $M1$ contributions. We reiterate that in our calculation non-zero E2/M1 ratios are uniquely due to non-valence degrees of freedom.

Table 1. Transition magnetic μ and quadrupole Q moments of decuplet baryons. The impulse and exchange current contributions from the PS meson cloud and the gluon and scalar quark-quark interactions to the transition magnetic moments are listed separately. The quadrupole PS-meson $Q_{\rm PS}$ and gluon-pair $Q_{\rm G}$ contributions are given individually. The last two columns contain the radiative decay widths Γ and $E2/M1$ ratios.

	$\mu_{\rm Imp}$ $[\mu_N]$	$\mu_{\rm PS}$ $[\mu_N]$	$\mu_{\rm G,Scal}$ $[\mu_N]$	$\mu_{\rm Tot}$ $[\mu_N]$	$Q_{\rm PS}$ [fm^2]	$Q_{\rm G}$ [fm^2]	Γ [keV]	$E2/M1$ [%]
$\gamma p \leftrightarrow \Delta^+$	2.828	.312	-.609	2.533	-.031	-.058	350	-3.65
$\gamma \Sigma^+ \leftrightarrow \Sigma^{*+}$	2.404	.029	-.166	2.267	-.040	-.051	105	-2.9
$\gamma n \leftrightarrow \Delta^0$	2.828	.312	-.609	2.533	-.031	-.058	350	-3.65
$\gamma \Sigma^0 \leftrightarrow \Sigma^{*0}$	-0.990	-.013	.078	-0.924	.013	.016	17.4	-2.3
$\gamma \Lambda \leftrightarrow \Sigma^{*0}$	2.449	.154	-.250	2.354	-.007	-.041	265	-2.0
$\gamma \Xi^0 \leftrightarrow \Xi^{*0}$	2.404	-.020	.044	2.428	-.004	-.035	172	-1.3
$\gamma \Sigma^- \leftrightarrow \Sigma^{*-}$	-0.424	-.004	.009	-0.419	.014	.018	3.61	-5.5
$\gamma \Xi^- \leftrightarrow \Xi^{*-}$	-0.424	.009	-.045	-0.460	.004	.012	6.18	-2.8

4 Octet hyperon charge radii

Constituent quarks are obtained through the dressing of current quarks by their strong interactions. For an electromagnetic probe they appear as extended objects. The cloud of the constituent quark is dominated by $q\bar{q}$ pairs with pseudoscalar meson quantum numbers. Guided by vector meson dominance, an electromagnetic constituent quark size can be assigned[2].

Our results[2] for the various one- and two-body contributions to the charge radii are given in Table 2. The experimental proton and neutron charge radii are well described within our model including gluon and PS-meson exchange currents.

In impulse approximation, $SU_F(3)$ symmetry breaking leads to a reduction of the charge radii with increasing strangeness content of the hyperon. As a consequence the proton, Σ^-, and Ξ^- have successively smaller charge radii. This strangeness suppression almost disappears when exchange currents are included. Due to the pseudoscalar meson cloud in the hyperons, the charge radius of the Σ^- (or Ξ^-) turns out to be almost as large as the proton charge radius. A similar trend may be indicated by the recent experimental results from SELEX presented at this conference[4]. SELEX obtain a Σ^- charge radius of $r^2_{\Sigma^-} = 0.60 \pm 0.08$ (stat) $\pm$ 0.08 (syst) fm^2, which agrees nicely with our result.

Table 2. Charge radii of octet hyperons. The PS-meson (π, K, η) and the gluon-pair $r^2_{\rm G}$ exchange currents are listed separately, as well as the scalar exchange current contributions.

	$r^2_{\rm Imp}$ [fm^2]	$r^2_{\rm PS}$ [fm^2]	$r^2_{\rm G}$ [fm^2]	$r^2_{\rm Scal}$ [fm^2]	$r^2_{\rm Tot}$ [fm^2]	$\sqrt{\lvert r^2_{\rm Tot}\rvert}$ [fm]
p	0.736	-0.057	0.123	-0.150	0.651	0.807
Σ^-	0.691	-0.028	0.054	-0.074	0.643	0.802
Ξ^-	0.633	-0.022	0.001	-0.025	0.587	0.766
Σ^+	0.861	-0.029	0.118	-0.125	0.826	0.909
n	0	-0.035	-0.082	0	-0.117	0.342
Σ^0	0.085	0.000	0.032	-0.028	0.088	0.296
Λ	0.085	-0.024	-0.014	-0.028	0.017	0.131
Ξ^0	0.169	-0.014	-0.034	-0.031	0.091	0.302

Acknowledgments

This work has been performed in collaboration with A. J. Buchmann and Amand Faessler (University of Tübingen, Germany). I thank the DFG for a postdoctoral fellowship WA1147/1-1.

References

1. G. Wagner, A. J. Buchmann, A. Faessler, *Phys. Rev.* C **58**, 1745 (1998).
2. G. Wagner, A. J. Buchmann, A. Faessler, *Phys. Rev.* C **58**, (1998), Dec. 1998.
3. J. S. Russ, *Nucl. Phys.* A **585**, 39c (1995); R. A. Schumacher, *Nucl. Phys.* A **585**, 63c (1995).
4. I. Eschrich for the SELEX Collaboration, these proceedings.
5. G. Wagner, A. J. Buchmann, A. Faessler, *Phys. Lett.* B **359**, 288 (1995).
6. A. J. Buchmann, these proceedings; A. J. Buchmann, E. Hernández, A. Faessler, *Phys. Rev.* C **55**, 448 (1997); A. J. Buchmann, E. Hernández, K. Yazaki, *Phys. Lett.* B **269**, 35 (1991).